

Crest-Factor Minimization Using Nonlinear Chebyshev Approximation Methods

Patrick Guillaume, *Member, IEEE*, Johan Schoukens, *Member, IEEE*, Rik Pintelon, *Member, IEEE*, and István Kollár, *Member, IEEE*

Abstract—Low crest-factor of excitation and response signals is desirable in transfer function measurements, since this allows the maximization of the signal-to-noise ratios (SNR's) for given allowable amplitude ranges of the signals. The paper presents a new crest-factor minimization algorithm for periodic signals with prescribed power spectrum. The algorithm is based on approximation of the nondifferentiable Chebyshev (minimax) norm by l_p -norms with increasing values of p , and the calculations are accelerated by using FFT's. Several signals related by linear systems can also be compressed simultaneously. The resulting crest-factors are significantly better than those provided by earlier methods. Moreover, it is shown that the peak value of a signal can be further decreased by allowing some extra energy at additional frequencies.

Keywords—Crest-factor, multisine, optimal excitation.

I. INTRODUCTION

TO experimentally determine the dynamic behavior of a linear time-invariant system, the input and output signals have to be measured. Measurements always introduce some errors depending upon the measurement method and the instrumentation used. By averaging the measurements it is possible to reduce the random errors while the systematic errors will usually persist. The sensitivity of the measurement process to disturbing noise is inversely proportional to the signal-to-noise ratio (SNR) of the measurements [1]. In many problems (e.g., control systems, biological systems) the choice of the excitation is very limited. However, in an important class of problems only the maximal values of the input and output signals, and some internal variables are restricted (to maintain the linear behavior of the device under test and/or to avoid overflow of the measurement equipment). This freedom can be used to design *optimal experiments* [3], [4], [8]–[10], [18]–[21], [24]–[26]. In most cases the aim of *experimental design* is to increase the SNR as much as possible.

The development in technology and the implementation of the fast Fourier transform (FFT) made it possible to

measure the spectrum of a signal in real-time (e.g., dynamic signal analyzers) instead of having to sweep (slowly) over the frequency range of interest (e.g., analog spectrum analyzers and network analyzers). In [25] ten different signals are studied to analyze their suitability as excitation signals for FFT-based signal and network analyzers. Their influence on the measurement time, the accuracy and the sensitivity to nonlinear distortion is analyzed. Schoukens *et al.* [25] conclude that multisines are universal, very flexible signals, that can be used to solve a lot of measurement problems in a minimum of time (a multisine is a signal obtained by the addition of a finite number of harmonically related sinusoids).

The crest-factor (CF) of a signal is defined as the ratio of its peak value and its root mean square (RMS) value. The number of averages required to measure a signal with a specified accuracy is proportional to the square of the crest-factor [25]. This demonstrates the importance of CF minimization in measurement problems. For instance, in quality control, the specifications of a lot of almost identical devices have to be verified. In such cases, the design of an optimal test signal having a low CF can result in an important gain of time and/or in an increase of accuracy.

The exact solution to CF minimization is still an open problem [3], [4], [10], [18]–[21], [24], [26]. In [19] an overview of the existing analytical and numerical methods is given for the compression of periodic signals. The time-frequency-domain swapping method presented in [19] is based on a generalization of the Gerchberg–Saxton algorithm. This algorithm allows the simultaneous compression of the input and output signals of single-input, single-output (SISO) systems. The extension of this algorithm to multi-input, multi-output (MIMO) systems for the simultaneous compression of the input and output signals is not possible in general (the input vector cannot always be written as a function of the output vector [10]). The new algorithm presented in this paper can handle the general MIMO problem. Further, it gives lower CF's and offers more possibilities.

The paper is organized as follows. The new algorithm is explained in Section II and the results are compared with the existing methods. In Section III the method is extended to allow the simultaneous compression of the input and output signals of a linear time invariant device, and the "snow effect" is introduced (by an adequate increase of the energy content of a signal, an extra decrease

Manuscript received January 14, 1991; revised November 6, 1991. This work was supported by the Belgian National Fund for Scientific Research (NFWO) and the Flemish Community (concerted action IMMI, IUAP 13).

P. Guillaume, J. Schoukens, and R. Pintelon are with the Department ELEC, Free University of Brussels, B-1050 Brussels, Belgium.

I. Kollár is with the Department of Measurement and Instrumentation Engineering, Technical University of Budapest, H-1521 Budapest, Hungary.

IEEE Log Number 9105626.

of the peak value can be obtained). The results are illustrated by examples. In Section IV, the conclusions are drawn.

II. CREST-FACTOR MINIMIZATION—THE L_∞ -METHOD

A. Preliminaries

A multisine x is a periodic signal with a band-limited spectrum. It can be represented by a Fourier series, i.e., a trigonometric sum of order K [13], [15], [23]

$$x(t) = \sum_{u=1}^{N_u} a_u \cos(2\pi k_u t/T + \alpha_u) \quad (1)$$

where k_u are the harmonic numbers ($k_u \in \mathbf{N}$, $u = 1, 2, \dots, N_u$) and $0 < k_1 < k_2 < \dots < k_{N_u} = K$.

Reference will be made to one of the most often used error criteria, namely the l_p -norm [2], [6], [13], [15], [23]. We begin with the following definitions.

Definition 1: The l_p -norm of the function $x(t)$ taken over the interval $[0, T]$ is denoted by $l_p(x)$ and is defined as

$$l_p(x) = \left[\frac{1}{T} \int_0^T |x(t)|^p dt \right]^{1/p}, \quad P \geq 1. \quad (2)$$

The mean absolute value (l_1 -norm) and the RMS value (l_2 -norm) are well known l_p -norms in the engineering literature. In addition to the l_p -norms, there is one other important and widely used norm, which is the Chebyshev norm (also known as the minimax norm, the uniform norm, or the maximum norm).

Definition 2: The Chebyshev norm $\|x\|_\infty$ of the continuous function $x(t)$ is defined as its peak value in the interval $[0, T]$:

$$\|x\|_\infty = \max_{t \in [0, T]} |x(t)|. \quad (3)$$

The Chebyshev norm is sometimes called the l_∞ -norm because of its relationship to the l_p -norm for very large values of p .

Definition 3: The crest-factor CF_x of the function $x(t)$ is given by

$$CF_x = l_\infty(x)/l_2(x). \quad (4)$$

In engineering terms, $l_\infty(x)$ is just the peak value of the signal x . In Section III a more general definition for the CF will be given.

B. Crest-Factor Minimization

Our problem consists of minimizing the CF of a multisine (1) with a given auto-power spectrum (i.e., the a_u are given constants). The parameters of the problem are for instance the phases α_u , $u = 2, 3, \dots, N_u$, with $\alpha_1 = 0$. Let us group these parameters in a vector \mathbf{p} with dimension $N_p \times 1$ ($N_p = N_u - 1$). Notice that the l_2 -norm (i.e., the RMS value) of a multisine is independent of the phases α_u , and thus, the CF minimization problem reduces to the minimization of the peak value of the mul-

tisine $l_\infty(x(\mathbf{p}, t))$ with respect to the phases in the vector \mathbf{p} . From the approximation theory standpoint, we try to make x as close to zero as possible using the Chebyshev norm as the distance function ($l_\infty(x(\mathbf{p}, t)) - 0$) is minimized [13], [15], [23]). Due to the equality constraints on the magnitude of the Fourier coefficients (a_u , $u = 1, 2, \dots, N_u$, are given constants), the multisine x cannot vanish to zero.

Formally, the problem can be stated as: find a real valued phase vector $\mathbf{p}_\infty \in \mathbf{R}^{N_p}$ such that the peak value of the corresponding multisine is the smallest among all the possible phases $\mathbf{p} \in \mathbf{R}^{N_p}$

$$l_\infty(x(\mathbf{p}_\infty, t)) \leq l_\infty(x(\mathbf{p}, t)), \quad \forall \mathbf{p} \in \mathbf{R}^{N_p}. \quad (5)$$

When the gradient exists, \mathbf{p}_∞ can be found as the solution of

$$\partial l_\infty(x(\mathbf{p}, t))/\partial \mathbf{p} = 0. \quad (6)$$

Formulation (6) is not suited for a straightforward calculation of \mathbf{p}_∞ since the Chebyshev norm is nondifferentiable. According to [2] the l_∞ -norm can be reformulated as an equivalent constrained differentiable minimization problem. From this constrained optimization problem, one concludes that an optimally compressed multisine can reach at most $N_p + 1$ times its peak value. However, due to the large number of variables, the application of this formulation to multisine compression is not practical [3], [20]. We still use in this paper another approach, which consists of minimizing the differentiable l_p -norm, where the index p is taken as a sequence such as 4, 8, 16, 32, 64 [6]. Using the Schroeder phase coding [26] as the starting value the l_4 -norm is minimized. The l_4 -solution \mathbf{p}_4 is used as the starting value for the next norm, and so on. This defines under some regularity conditions a descent algorithm that converges to the minimax solution \mathbf{p}_∞ if the best l_p -approximations \mathbf{p}_p were found (Pólya's algorithm [6], [23]):

$$\lim_{p \rightarrow \infty} \mathbf{p}_p = \mathbf{p}_\infty. \quad (7)$$

Due to the nonlinear appearance of the phases \mathbf{p} in the multisine x , we are faced with the problem of local minima. However, from experience, we observed that the method described in this paper generates better results than the existing CF minimization methods.

C. The L_p -Error Criterion

In numerical work it is convenient to use a simpler discrete error criterion

$$L_p(x_n) = \frac{1}{N} \sum_{n=0}^{N-1} |x_n|^p \quad (8)$$

with $x_n = x(t_n)$. We note here that the points t_n need not be equally spaced. However, choosing $t_n = nT/N$ has some definite advantages. In Appendix A it is proven that $L_p(x_n) = [l_p(x)]^p$ for even values of p and $t_n = nT/N$ if $N > pK + 1$. Hence, if the conditions of Appendix A are

fulfilled, the discrete L_p -norm and the continuous l_p -norm are equivalent. If these conditions are not satisfied, the discrete norm is only an approximation of the continuous one. In Appendix B a lower and upper bound have been derived for the Chebyshev norm of a sampled trigonometric polynomial.

D. The Gauss-Newton Algorithm

As we have seen above, our task reduces to the minimization of the multivariate nonlinear function $L_p(x_n)$. A lot of methods exist to tackle this problem [7], [12], [16]. We will use the Gauss-Newton algorithm in combination with Levenberg-Marquardt. Equation (8) then has to be rewritten as

$$L_p(x_n) = \frac{1}{N} \mathbf{e}^T \mathbf{e} \tag{9}$$

where \mathbf{e} is a column vector with N entries $e_n = x_n^q$, $n = 0, 1, \dots, N - 1$, and $q = p/2$ with p even. Only first-order derivatives are required, which in our case are readily obtained. The Jacobian matrix \mathbf{J} , which is defined as

$$J_{nu} = \partial e_n / \partial \alpha_u \tag{10}$$

becomes

$$J_{nu} = -q x_n^{q-1} a_u \sin(2\pi k_u t_n / T + \alpha_u). \tag{11}$$

Using \mathbf{e} and \mathbf{J} as defined above, the Gauss-Newton iterative algorithm can be formulated as

$$\mathbf{p}^{(i)} = \mathbf{p}^{(i-1)} - [\mathbf{J}^{(i-1)T} \mathbf{J}^{(i-1)} + \mathbf{\Lambda}^{(i-1)}]^{-1} \mathbf{J}^{(i-1)T} \mathbf{e}^{(i-1)} \tag{12}$$

with $\mathbf{\Lambda}^{(i-1)}$ a positive-definite Levenberg-Marquardt matrix [12], [16]. The upper indexes between parentheses stand for the iteration number. In Appendix C, a time-efficient algorithm, based on the FFT, is given to compute $\mathbf{J}^{(i-1)T} \mathbf{J}^{(i-1)}$ and $\mathbf{J}^{(i-1)T} \mathbf{e}^{(i-1)}$.

E. Results

Example 1: Take a multisine consisting of 31 components with equal magnitudes ($a_u = 1$; $k_u = 1, 2, \dots, 31$). The Schroeder solution [26] gives a CF (4) of 1.782, the time-frequency-domain swapping algorithm gives a crest-factor of 1.405 [19] and the L_∞ -method's CF is 1.393 (Fig. 1). In Fig. 2, the computation times needed for the swapping algorithm (2048-point FFT) and the L_∞ -algorithm are compared. Both methods were implemented in MatLab on a Macintosh II (MC68020, 68881 floating-point coprocessor, 16-MHz clock). Fig. 3 shows the evolution of the CF and the corresponding computation time as a function of the maximal number of time samples N used in the L_p -error criterion. Notice that $N \approx 32 K$ is already large enough to obtain a good compression.

Example 2: Consider a multisine with 100 components ($a_u = 1$; $k_u = 1, 2, \dots, 100$). In Fig. 4 the computation times needed for the swapping algorithm (4096-point FFT) and the L_∞ -algorithm are compared.

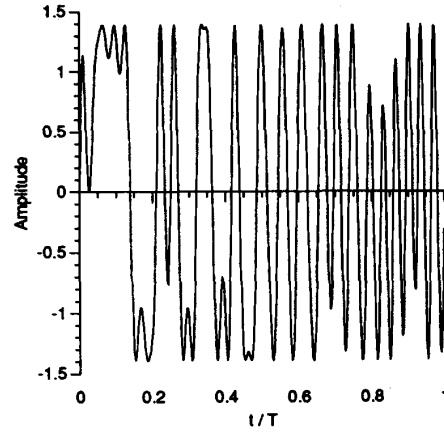


Fig. 1. Compressed multisine with 31 harmonics.

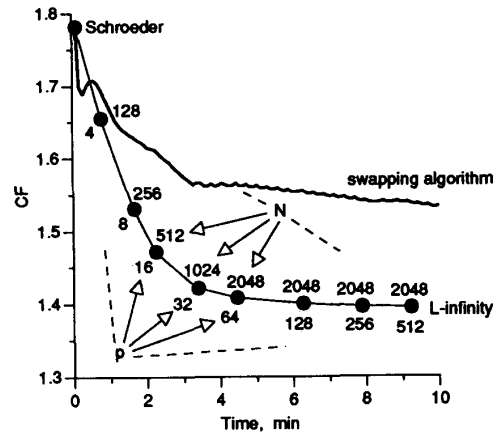


Fig. 2. Evolution of the crest-factor versus the time for the swapping algorithm (—) and the L_∞ -algorithm (●).

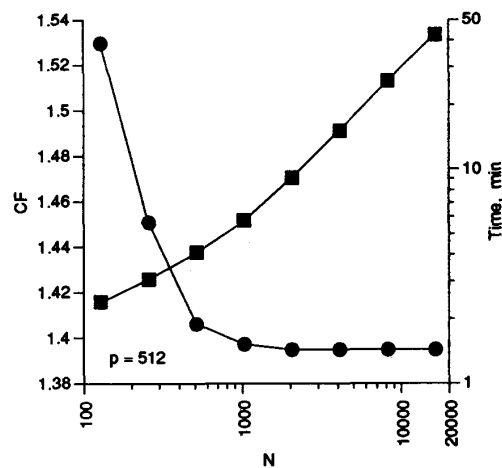


Fig. 3. Evolution of the crest-factor (●) and the computation time (■) versus the number of time samples N .

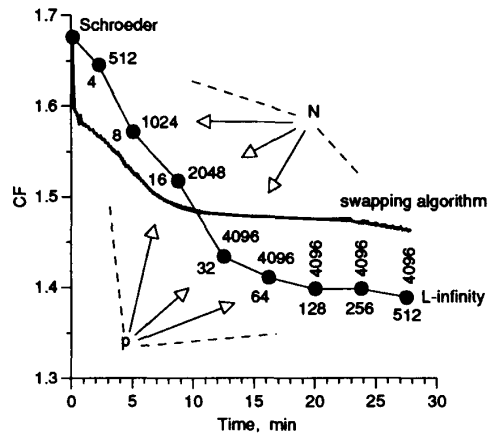


Fig. 4. Evolution of the crest-factor versus the time for the swapping algorithm (—) and the L_∞ -algorithm (●).

Example 3: Consider a logtone multisine with 13 equal-magnitude components ($a_u = 1$; $k_u = 10, 12, 15, 18, 22, 27, 33, 40, 48, 58, 70, 84, 100$). The Schroeder solution gives a CF of 3.19, the swapping algorithm crest-factor is 2.32 (4096-point FFT, 50 min.) and that of the L_∞ -method is 1.96 ($N = 4096$, 50 min.).

Example 4: Consider a multisine with 16 components ($a_u = \sin \pi(2k_u - 1)/32$; $k_u = 1, 2, \dots, 16$). For this problem, Van den Bos finds a CF of 1.51 [3]. With the L_∞ -method, one obtains 1.42 ($N = 2048$) as the CF.

F. Discussion

The idea of using standard optimization techniques based on a cost function approach to design low-CF signals is not new [4], [14], [20]. None of the previous trials, however, has resulted in a usable method. This is mainly due to the very complicated phase dependency of the CF, resulting in a cost function with many local minima. In [4], it was observed that a descent routine, started from Newman's phases, converged to a local minimum, yielding a minimal decrease in the CF. Global optimization routines can be used to avoid the local minima. However, these algorithms are in general very time-consuming [7]. Therefore, alternative methods were developed which circumvent the cost function optimization problem (e.g., [3] and [19]). Regardless of the above remarks, the method presented is again based on a cost function approach. Seemingly, by using Pólya's algorithm to approximate the best Chebyshev solution, one avoids many of the local minima. In all the tests we made, we were able to find lower CF's than the existing methods, although there is no guarantee that the algorithm converges to a global minimum.

III. GENERALIZATIONS OF THE L_∞ -METHOD

A. Input-Output Crest-Factor Optimization

To compress the input and output signals of a linear time-invariant device simultaneously, a new cost function

has to be constructed in such a way that the Chebyshev norms of the input and output signals are minimized at the same time. Consider the following definitions.

Definitions 4: The common L_p -norm of the functions $x(t)$ and $y(t)$ taken over the interval $[0, T]$ is denoted by $l_p(x, y)$ and is defined as

$$l_p(x, y) = \left[\frac{1}{2T} \int_0^T (|x(t)|^p + |y(t)|^p) dt \right]^{1/p}, \quad (13)$$

$$p \geq 1.$$

Definition 5: The common Chebyshev norm $\|x, y\|_\infty$ of the continuous functions $x(t)$ and $y(t)$ is a scalar defined as the largest peak value of $x(t)$ and $y(t)$ over the interval $[0, T]$

$$\|x, y\|_\infty = \max_{t \in [0, T]} \max (|x(t)|, |y(t)|). \quad (14)$$

The algorithm described in the previous section can easily be modified to minimize the Chebyshev norm (14) of the input and output signals. Notice that the output signal of a linear time-invariant dynamic system is given by

$$y(t) = \sum_{u=1}^{N_u} a_u G_u \cos(2\pi k_u t/T + \alpha_u + \phi_u) \quad (15)$$

with G_u and ϕ_u , respectively, the *a priori* known gain and phase shift introduced by the transfer function of the system at spectral line k_u . The parameters of the problem are still the phases α_u . Define two vectors \mathbf{e}_x and \mathbf{e}_y as $\mathbf{e}_{xn} = x_n^q$ and $\mathbf{e}_{yn} = y_n^q$, respectively, ($q = p/2$ with p even). Replace \mathbf{e} ($= \mathbf{e}_x$) in (9) by $\mathbf{e} = [\mathbf{e}_x^T, \mathbf{e}_y^T]^T$. According to [11], the algorithm converges to a solution which minimizes (14). Usually, equal extreme peak values of the input and output signals are obtained. Other solutions are possible by the introduction of weighting factors, i.e., by minimization of $\|x/w_x, y/w_y\|_\infty$. When the weighting factors w_x and w_y are proportional to the RMS values, signals with equal CF's are obtained. One can notice, for instance, that when the *peak ratio* $r = w_y/w_x$ is chosen too large (e.g., when $r > y_{WC}/x_{RMS}$ with $y_{WC} = \sum_u |a_u G_u|$ the worst case peak value) the problem reduces to the minimization of $\|x\|_\infty$.

Example 5: Given a linear system with transfer function

$$H(s) = \frac{s}{s^3 + 2s^2 + 2s + 1}. \quad (16)$$

Take as the excitation the same multisine as in Example 1 ($a_u = 1$; $s_u = 0.0625jk_u$; $k_u = 1, 2, \dots, 31$). The weighting factors are chosen proportional to the RMS values (the peak ratio r equals 0.5). The results are shown in Fig. 5. The CF's of the input and output signals are both 1.59, while the amplitude range of the output signal is 0.5 times the amplitude range of the input signal.

Example 6: When equal weighting factors are used in Example 5 ($r = 1$), the CF of the input signal becomes 1.393, while the CF of the output signal equals 2.197. Notice in Fig. 6 that the output signal does not reach the

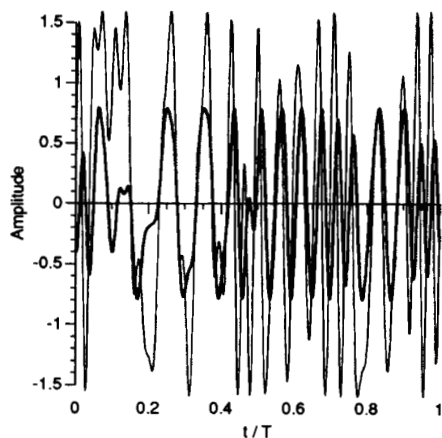


Fig. 5. Compressed input (—) and output (---) multisines with $r = 0.5$ (equal crest-factors).

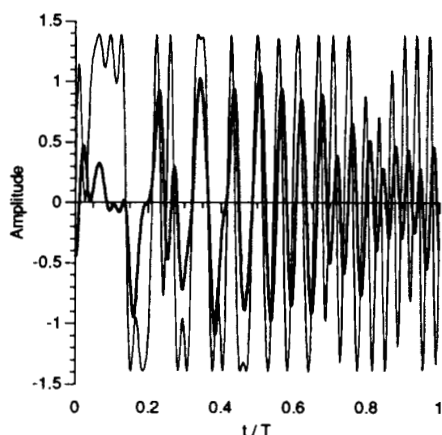


Fig. 6. Compressed input (—) and output (---) multisines with $r = 1$.

peak value, i.e., $\|x, y\|_\infty = \|x\|_\infty$ (the peak ratio r is too large). Compare with Fig. 1 and notice that both input signals are identical.

B. Multi-Input, Multi-Output Crest-Factor Optimization

The output signals of a linear MIMO system are given by

$$y_i(t) = \sum_{j=1}^{N_i} \sum_{u=1}^{N_u} a_{ju} G_{iju} \cos(2\pi k_u t/T + \alpha_{ju} + \phi_{iju}) \quad (17)$$

with $i = 1, 2, \dots, N_o$. N_i is the number of inputs and N_o the number of outputs. G_{iju} represents the gain and ϕ_{iju} the phase shift introduced by the transfer function between output i and input j of the MIMO system at spectral line k_u , $k_u = 1, 2, \dots, N_u$. The parameters of the problem are the phases α_{ju} . Following the same reasoning as in Section III.A, the Chebyshev norm $\|x_1/w_{x1}, \dots, x_{N_i}/w_{xN_i}, y_1/w_{y1}, \dots, y_{N_o}/w_{yN_o}\|_\infty$ is minimized.

Example 7: Consider a linear time-invariant dynamic MIMO system with transfer function matrix

$$H(s) = \frac{1}{s^3 + 2s^2 + 2s + 1} \begin{bmatrix} s & 1 \\ 1 & s + 1 \end{bmatrix}. \quad (18)$$

Input signals with the same specifications as the multisine in Example 5 are used. When choosing the RMS values as weighing factors, the algorithm produces multisines with CF's equal to 1.61.

C. The "Snow Effect"

We will demonstrate that an adequate increase of the energy content of a signal can result in an extra decrease of its peak value [10]. Consider

$$x(t) = \sum_{u=1}^{N_u} a_u \cos(2\pi k_u t/T + \alpha_u) + \sum_{s=1}^{N_s} b_s \cos(2\pi \tilde{k}_s t/T + \beta_s) \quad (19)$$

with $\tilde{k}_s \neq k_u \forall s, u$. The parameters of the optimization problem are now α_u , b_s , and β_s . The results of Appendix C can easily be extended for the new parameters.

The term *useful spectral lines* (k_u ; $u = 1, 2, \dots, N_u$) is used here to denote the spectral lines the experimenter selected to excite the device under test. The values of the coefficients a_u are specified by the experimenter (e.g., an optimal amplitude spectrum [8]–[10], [20], [24]). The terms *additional spectral lines* and *snow lines* (\tilde{k}_s ; $s = 1, 2, \dots, N_s$; $\tilde{k}_s \neq k_u$) denote the spectral lines which were added to the original design to obtain a better CF. The spectrum of the additional lines is determined completely by the CF optimization algorithm.

Notice that the previous definition of the CF (4) has to be modified. To obtain an honest comparison criterion, only the RMS value of the useful spectral lines (k_u ; $u = 1, 2, \dots, N_u$) should be taken into account.

Definition 6: The crest-factor CF_x of a trigonometric polynomial $x(t)$ with useful harmonics k_u ; $u = 1, 2, \dots, N_u$, is given by

$$CF_x = l_\infty(x) / x_{RMSu} \quad (20)$$

with $x_{RMSu} = \sqrt{\sum_{u=1}^{N_u} a_u^2 / 2}$ the RMS value of only the useful harmonics.

Example 8: Consider again the multisine of Example 1 ($a_u = 1$; $k_u = 1, 2, \dots, 31$) with 31 snow lines ($\tilde{k}_s = 32, 33, \dots, 62$). The CF (20) becomes 1.25 (Fig. 7).

Example 9: Consider the logtone of Example 3. By adding snow lines between the useful lines, a significant decrease of the amplitude range is observed (Fig. 8). The CF (20) equals 1.54.

Example 10: The results of the input-output compression problem given in Example 5 can also be ameliorated by the addition of snow lines ($\tilde{k}_s = 32, 33, \dots, 124$). The results are summarized in Fig. 9. The CF (20) equals 1.44.

IV. CONCLUSIONS

The new method proposed in this paper minimizes the CF of multisines with an arbitrary user-defined auto-power

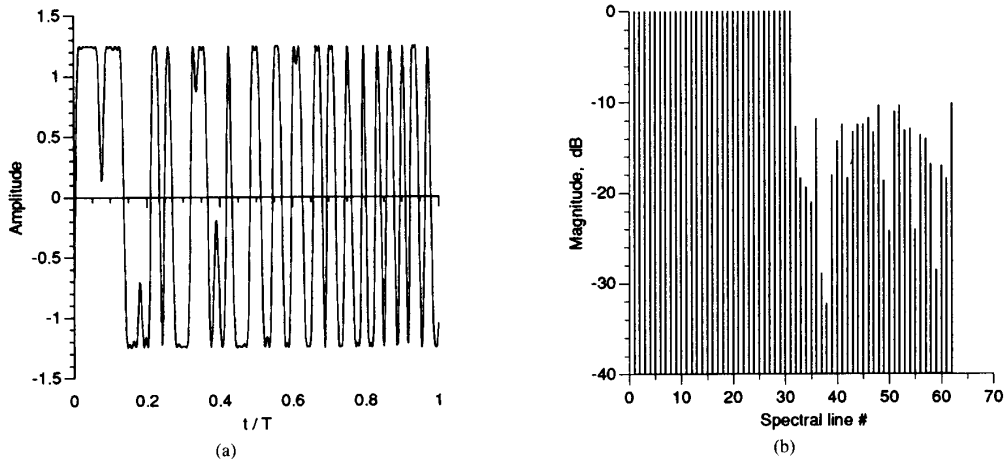


Fig. 7. Compressed multisine with snow lines: (a) time-domain. (b) frequency-domain.

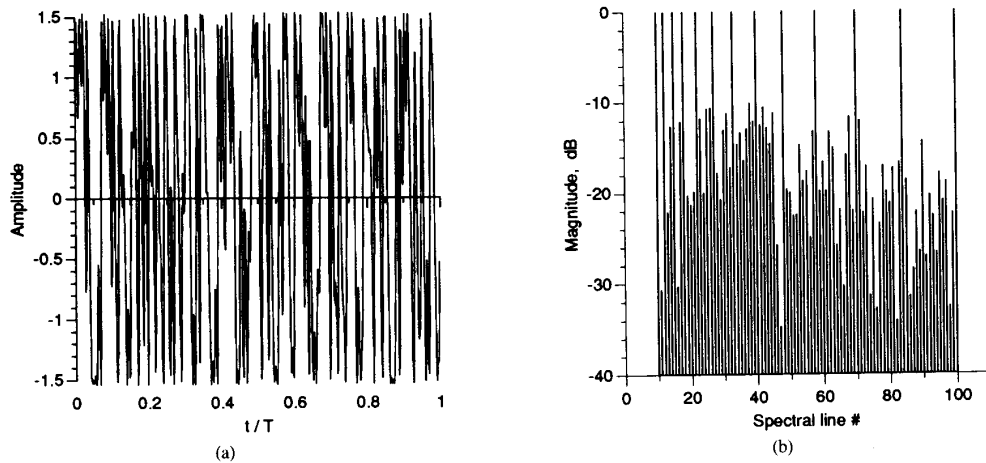


Fig. 8. Compressed logtone with snow lines between the useful lines. (a) time-domain. (b) frequency-domain.

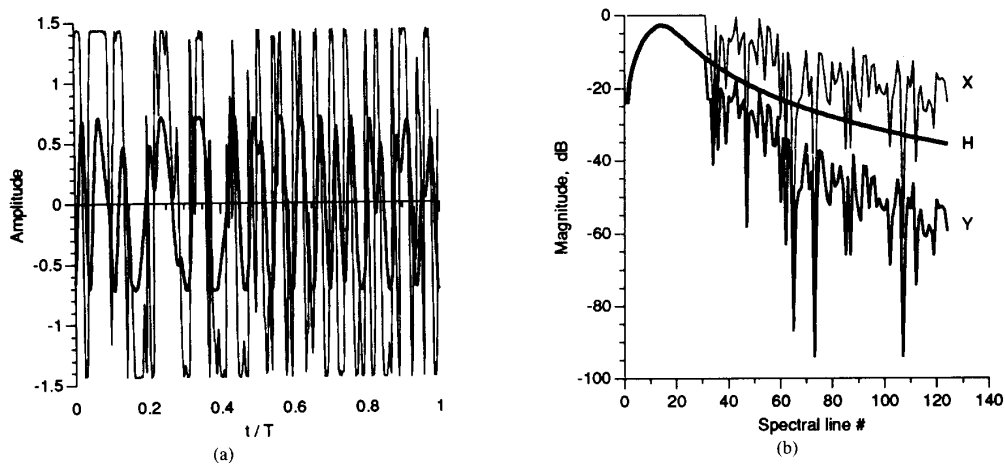


Fig. 9. Compressed input and output multisines with snow lines. (a) time-domain (—: input signal; - - -: output signal). (b) frequency-domain (X: input spectrum; Y: output spectrum; H: transfer function).

spectrum. It also allows the simultaneous compression of multisines related by linear time-invariant dynamic MIMO systems. Notice that an *a priori* knowledge of the dynamics of the linear device under test is necessary to simultaneously optimize the input and output signals. Minor inaccuracies in this knowledge do not have important consequences. In all cases investigated, the new method was able to produce multisines with lower CF's than those of the conventional methods.

The algorithm can efficiently be implemented by means of the fast Fourier transform. By the addition of snow lines an extra decrease of the peak value can be obtained. An important advantage of the method with respect to those described in the literature is its ability to design excitation signals adapted to the limited measurement ranges of the data acquisition channels used. This requirement is necessary to allow an optimal use of the measurement ranges, resulting in maximal SNR's.

APPENDIX A

Lemma 1: The discrete L_p -norm of the sampled trigonometric polynomial $x_n = x(t_n)$ and the continuous l_p -norm of the trigonometric polynomial $x(t)$ are equivalent for even values of p and $t_n = nT/N$ (i.e., $L_p(x_n) = [l_p(x)]^p$) if $N > pK + 1$ with K the order of the trigonometric polynomial.

Proof: Consider

$$x(t) = \sum_{u=1}^{N_u} a_u \cos(2\pi k_u t/T + \alpha_u). \quad (21)$$

The square of x equals

$$\begin{aligned} x^2(t) &= \sum_{u=1}^{N_u} \sum_{v=1}^{N_u} a_u a_v C_u C_v \\ &= \sum_{u=1}^{N_u} \sum_{v=1}^{N_u} a_u a_v (C_{u+v} + C_{u-v})/2 \end{aligned} \quad (22)$$

with $C_u = \cos(2\pi k_u t/T + \alpha_u)$ and $C_{u \pm v} = \cos(2\pi(k_u \pm k_v)t/T + \alpha_u \pm \alpha_v)$.

In general, taking the p th power of a trigonometric signal x of order K will generate a trigonometric signal of order pK :

$$x^p(t) = \sum_{k=0}^{pK} A_k \cos(2\pi kt/T) + \sum_{k=1}^{pK} B_k \sin(2\pi kt/T). \quad (23)$$

Integration over one period causes all time dependent terms to vanish. Only A_0 remains (which is a function of a_u and α_u [14])

$$A_0 = \frac{1}{T} \int_0^T x^p(t) dt. \quad (24)$$

It is well known that when the Nyquist condition is fulfilled the exact Fourier coefficients can be obtained from a finite set of data points [22], [27]. If the Nyquist con-

dition is not satisfied, aliasing occurs. The DC-component

$$A_0 = \frac{1}{N} \sum_{n=0}^{N-1} x_n^p \quad (25)$$

will not be altered if $N > pK + 1$.

From (24) and (25) one proves that $L_p(x_n) = [l_p(x)]^p$ for even values of p .

APPENDIX B

From Appendix A, it follows that the exact computation of the Chebyshev norm of a trigonometric polynomial x , and thus, the CF, requires an infinite amount of samples x_n . When a finite number of samples is used, lower and upper bounds of the Chebyshev norm can be specified. The lower bound is given by

$$\|x\|_L = \max_n |x_n|. \quad (26)$$

Proof: $\|x\|_L = \max_n |x_n| \leq \max_t |x(t)| = \|x\|_\infty$.

The upper bound can be obtained by the inequality of Bernstein [13].

Theorem 1: If a trigonometric polynomial $T_K(\theta)$ of period 2π and order K satisfies the inequality $|T_K(\theta)| \leq M$, then

$$|\partial T_K(\theta)/\partial \theta| \leq KM, \quad \forall \theta. \quad (27)$$

Using Theorem 1, we prove that

$$\|x\|_U = \frac{\|x\|_L}{1 - K\pi/N}, \quad N > K\pi \quad (28)$$

is an upper bound of the Chebyshev norm with N the number of equidistant samples in a period T .

Proof: The proof is based on the fact that $\|x\|_\infty$ is smaller than $\|x\|_L$ plus the largest derivative of x times the interval between the samples divided by 2.

$$\|x\|_\infty < M = \|x\|_L + MK \times \pi/N. \quad (29)$$

With $M = \|x\|_U$, (28) is proven.

APPENDIX C

The normal equations can efficiently be constructed by means of the FFT-algorithm. With the notations of Appendix A

$$C_u = \cos(2\pi k_u n/N + \alpha_u) \quad (30)$$

$$S_u = \sin(2\pi k_u n/N + \alpha_u). \quad (31)$$

The matrix $\mathbf{J}^T \mathbf{J}$ becomes ($q = p/2$ with p even)

$$[\mathbf{J}^T \mathbf{J}]_{uv} = q^2 \sum_{n=0}^{N-1} x_n^{2q-2} a_u a_v S_u S_v \quad (32)$$

$$= p^2 \sum_{n=0}^{N-1} x_n^{p-2} a_u a_v (C_{u+v} - C_{u-v})/8 \quad (33)$$

$$= p^2 \operatorname{Re}(\psi_{u-v,p-2} - \psi_{u+v,p-2})/8 \quad (34)$$

with

$$\psi_{u \pm v, p-2} = a_u a_v e^{-j(\alpha_u \pm \alpha_v)} X_{k_u \pm k_v, p-2}$$

and

$$X_{k_u \pm k_v, p-2} = \sum_{n=0}^{N-1} x_n^{p-2} \exp[-j2\pi(k_u \pm k_v)n/N].$$

Notice that $X_{k, p-2} = \sum_{n=0}^{N-1} x_n^{p-2} e^{-j2\pi kn/N}$ is the discrete Fourier transform (DFT) of the sequence x_n^{p-2} , $n = 0, 1, \dots, N-1$. In a similar way, the vector $\mathbf{J}^T \mathbf{e}$ can be rewritten as

$$[\mathbf{J}^T \mathbf{e}]_u = -q \sum_{n=0}^{N-1} x_n^{2q-2} \sum_{v=1}^{N_u} a_u a_v S_u C_v \quad (35)$$

$$= p \sum_{v=1}^{N_u} \text{Im}(\psi_{u-v, p-2} + \psi_{u+v, p-2})/4. \quad (36)$$

REFERENCES

[1] J. S. Bendat and A. G. Piersol, *Engineering Applications of Correlation and Spectral Analysis*. New York: John Wiley & Sons, 1980.
 [2] A. Van den Bos, "Nonlinear least-absolute-values and minimax model fitting," presented at the 7th IFAC Symposium on Identification and System Parameter Estimation, July 3-7, 1985, York, UK.
 [3] A. Van den Bos, "A new method for synthesis of low-peak-factor signals," *IEEE Trans. Acoust., Speech, Sig. Process.*, vol. ASSP-35, pp. 120-122, Jan. 1987.
 [4] S. Boyd, "Multitone signals and low crest factor," *IEEE Trans. Circuits Syst.*, vol. CAS-33, pp. 1018-1022, Oct. 1986.
 [5] L. O. Chua, "Global optimization: A naive approach," *IEEE Trans. Circuit Theory*, vol. CT-37, pp. 966-969, July 1990.
 [6] A. G. Deczky, "Synthesis of recursive digital filters using the minimum p-error criterion," *IEEE Trans. Audio Electroacoust.*, vol. AU-20, pp. 257-263, Oct. 1972.
 [7] L. C. W. Dixon and G. P. Szegö, *Towards Global Optimization*. North-Holland Publishing Company, 1975.
 [8] V. V. Fedorov, *Theory of Optimal Experiments*. New York: Academic Press, 1972.
 [9] G. C. Goodwin and R. L. Payne, *Dynamic System Identification: Ex-*

perimental Design and Data Analysis. New York: Academic Press, 1977.
 [10] P. Guillaume, I. Kollár, and J. Schoukens, "On the design of optimal input signals for multi-input, multi-output system identification," in *Proceedings of the 15th International Seminar on Modal Analysis*, pp. 1223-1239, 1990.
 [11] P. Guillaume, "Generalization of Pólya's algorithm," Internal note, Vrije Universiteit Brussel, Dept. ELEC, Brussels, Belgium, Dec. 1990.
 [12] A. Iserles and M. J. D. Powell, *The State of the Art in Numerical Analysis*. Oxford, UK: Clarendon Press, 1987.
 [13] G. G. Lorentz, *Approximation of Functions*. New York: Chelsea Publishing Company, 1986.
 [14] P. Matthys, J. Renneboog, L. Auwaerts, and J. Schoukens, "Signal generation with minimal crest factor," presented at the IMEKO Symp. on Measurement and Estimation, Bressanone, Brixen, 1984.
 [15] G. Meinardus, *Approximation of Functions: Theory and Numerical Methods*. New York: Springer-Verlag, 1967.
 [16] J. P. Norton, *An Introduction to Identification*. New York, Academic Press, 1986.
 [17] A. V. Oppenheim and R. W. Schaffer, *Digital Signal Processing*. New York, Prentice-Hall, 1975.
 [18] E. Van der Ouderaa, J. Schoukens, and J. Renneboog, "Peak factor minimization using a time-frequency domain swapping algorithm," *IEEE Trans. Instrum. Meas.*, vol. IM-37, pp. 145-147, March 1988.
 [19] E. Van der Ouderaa, J. Schoukens, and J. Renneboog, "Peak factor minimization of input and output signals of linear systems," *IEEE Trans. Instrum. Meas.*, vol. IM-37, pp. 207-212, June 1988.
 [20] E. Van der Ouderaa, "Design of optimal input signals with minimal crest factor," Ph.D. thesis, Vrije Universiteit Brussel, Dept. ELEC, Brussels, Belgium, Nov. 1988.
 [21] E. Van der Ouderaa and J. Renneboog, "Logtone crest factors," *IEEE Trans. Instrum. Meas.*, vol. IM-37, pp. 656-657, Dec. 1988.
 [22] L. R. Rabiner and B. Gold, *Theory and Application of Digital Signal Processing*. New York: Prentice-Hall, 1975.
 [23] J. R. Rice, *The Approximation of Functions*. Reading, MA: Addison-Welley, 1964.
 [24] J. Schoukens, P. Guillaume, and R. Pintelon, "Design of multisine excitations," presented at the IEE Control 91 Conference, March 25-28, 1991, Edinburgh, Great Britain.
 [25] J. Schoukens, R. Pintelon, E. Van der Ouderaa, and J. Renneboog, "Survey of excitation signals for FFT based signal analyzers," *IEEE Trans. Instrum. Meas.*, vol. IM-37, pp. 342-352, Sept. 1988.
 [26] M. R. Schroeder, "Synthesis of low peak factor signals and binary sequences with low autocorrelation," *IEEE Trans. Inform. Theory*, vol. IT-16, pp. 85-89, 1970.
 [27] M. Schwartz and L. Shaw, *Signal Processing: Discrete Spectral Analysis, Detection, and Estimation*. New York: McGraw-Hill, 1975.